

Role of hyperfine and anisotropic exchange interaction in the exciton luminescence of quantum dots

© D.S. Smirnov, E.L. Ivchenko

Ioffe Institute, St. Petersburg, Russia

smirnov@mail.ioffe.ru

Received May 25, 2024

Revised May 25, 2024

Accepted August 01, 2024

Optical orientation and alignment of excitons in semiconductor indirect band gap quantum dots were studied theoretically. The study examines a special mode in which the energy of hyperfine interaction between an electron and lattice nuclei is low compared with the exchange splitting between bright and dark exciton levels, but is comparable with the anisotropic exchange splitting of a radiative doublet. Dependences of degrees of circular and linear polarization on an external magnetic field during resonance excitation of excitons by polarized light were calculated.

Keywords: quantum dots, polarized luminescence, optical exciton spectroscopy, hyperfine interaction, nanophotonics.

DOI: 10.61011/EOS.2024.08.60033.6714-24

1. Introduction

Several parameters affect the polarization of exciton luminescence excited in semiconductor quantum dots by polarized optical radiation: exchange splitting δ_0 between radiative and nonradiative doublets, anisotropic exchange splitting of each of these doublets, respectively, δ_b and δ_d [1], radiative and nonradiative lifetimes, τ_r and τ_{nr} , and energy of hyperfine interaction between an electron and lattice nuclei, ε_N . In quantum dots grown on the basis of direct-band-gap semiconductors, ε_N is low compared with δ_0 and \hbar/τ_r , and nuclear spins don't affect bright exciton photoluminescence in magnetic fields at which the Zeeman splitting ε_B of exciton sublevels is low compared with δ_0 . Study [2] investigated the polarized photoluminescence in indirect band gap quantum dots in a special mode where the exchange splitting δ_0 , hyperfine interaction energy ε_N and radiative broadening \hbar/τ_r are comparable in the order of magnitude and, therefore, the Overhauser field induced by nuclear spins plays an important role. This mode is hereinafter denoted by a Roman numeral I. There is another special exciton luminescence mode (mode II) where $\delta_0 \gg \varepsilon_N, \varepsilon_B$, but relations between $\hbar/\tau_r, \varepsilon_N, \delta_b$ and ε_B are arbitrary. According to [3,4], the linear dimension scatter in the (In,Al)As/AlAs quantum dot array makes coexistence of modes I and II possible for different dots in the same sample. This study addresses exciton luminescence mode II that hasn't been investigated theoretically before.

Importance of this field of study is associated with the explosive development of quantum technologies based on the entanglement phenomenon. Quantum dots make it possible to generate and examine entangled photon pairs in biexciton cascade recombination [5–8], in particular, to verify experimentally the Bell inequalities [9]. The degree of entanglement of two photons is defined by the exciton fine

structure [10] and may be limited exactly by the hyperfine interaction when $\delta_b < \varepsilon_N$ [11–13]. However, as mentioned above, $\hbar/\tau_r \gg \varepsilon_N$ is satisfied in ordinary quantum dots, for example, InGaAs/GaAs, and the nuclear effect is low in them. It will be shown that in mode II with $\varepsilon_B \ll \delta_0$ when mixing of bright and dark excitons may be neglected, luminescence polarization may be, nevertheless, controlled by the hyperfine interaction. A case of stronger magnetic fields at which the Zeeman splitting ε_B exceeds $\delta_b, \varepsilon_N, \hbar/\tau_r$, is comparable with δ_0 and ensures intersection of bright and dark exciton sublevels is addressed in the second part of the work.

2. Exciton Hamiltonian

A radiative exciton doublet localized in the AlAs/AlGaAs quantum dot and formed by an electron in valley X and hole in the vicinity of center Γ of the Brillouin zone is addressed. The presence of a quantum dot boundary provides addition of the Bloch states to the X-electron wave function in the vicinity of the Γ -dot and, consequently, zero-phonon exciton luminescence also occurs, besides the phonon luminescence. When the exchange splitting δ_0 is high and exciton spin relaxation is neglected, dark exciton states don't occur. Further, a laboratory coordinate system x_0, y_0, z is set up with the z axis along the structure growth axis. Moreover, the lateral x, y coordinates are introduced for each of the quantum dots in accordance with its anisotropy.

Two $|+1\rangle$ and $| -1\rangle$ exciton sublevels that are optically active in the σ^+ and σ^- polarizations may be conveniently described in the pseudospin description method [14]. Hamiltonian describing the exciton level fine structure is

generally written as

$$\mathcal{H} = \frac{1}{2} \hbar \Omega \cdot \boldsymbol{\sigma}. \quad (1)$$

Here, $\boldsymbol{\sigma}$ is the vector of the Pauli matrices in this basis, Ω is the effective Larmor pseudospin precession frequency with three components Ω_i , $i = 1, 2, 3$. Ω_1 and Ω_2 result from the localizing potential anisotropy taking into account the long-range exchange interaction [5–20]. δ_b defined in the introduction is obviously equal to $\hbar \sqrt{\Omega_1^2 + \Omega_2^2}$. The third component is

$$\Omega_3 = \Omega_N + \Omega_B, \quad (2)$$

where Ω_N is associated with the nuclear spin fluctuation action of the crystalline lattice, and Ω_B is equal to $g_{\parallel} \mu_B B_z / \hbar$, where g_{\parallel} is the longitudinal g -factor of exciton, μ_B is the Bohr magneton, B_z is the z -component of the magnetic field \mathbf{B} . Lateral components of the magnetic field \mathbf{B} and the Overhauser field in linear approximation are not included in Hamiltonian (1). A case of quite weak magnetic fields where $\hbar \Omega_B \ll \delta_0$ is considered hereinafter.

Hyperfine spin interaction of the electron \mathbf{S} and hole \mathbf{J} with nuclei is short-range and may be written as

$$\mathcal{H}_{hf} = v_0 \sum_n [\hat{\mathbf{S}} \hat{\mathbf{A}}_e \mathbf{I}_n \delta(\mathbf{r}_e - \mathbf{R}_n) + \hat{\mathbf{J}} \hat{\mathbf{A}}_h \mathbf{I}_n \delta(\mathbf{r}_h - \mathbf{R}_n)], \quad (3)$$

where n enumerates the nuclear spins \mathbf{I}_n located at the crystalline lattice sites \mathbf{R}_n , v_0 is the lattice cell volume, $\mathbf{r}_{e,h}$ are the electron and hole radius vectors in the smooth envelope method, $\hat{\mathbf{A}}_{e,h}$ are the energy-dimension hyperfine interaction tensors that, for simplicity, are assumed equal for all nuclei. Due to the time reversal symmetry, the electron and hole states of interest in the quantum dot may be considered as described by the real envelopes of wave functions $\Phi_e(\mathbf{r}_e)$, $\Phi_h(\mathbf{r}_h)$. Single-particle size quantization energy is assumed to be higher than the exciton rydberg. Then the longitudinal nuclear field applied to the exciton is given by

$$\hbar \Omega_N = v_0 \sum_n [A_h \Phi_h^2(\mathbf{R}_n) - A_e \Phi_e^2(\mathbf{R}_n)] I_{n,z}, \quad (4)$$

where $A_e = A_{e;zz}$, $A_h = 3A_{h;zz}$ and the off-diagonal tensor components \hat{A}_e and \hat{A}_h are taken to be equal to zero. This takes into account that the $|\pm 1\rangle$ exciton state is formed by a hole with a spin of $\pm 3/2$ and an electron with a spin of $\mp 1/2$.

In our opinion, nuclear spin dynamics occurs at times that are much longer than the exciton lifetime, and the dynamic nuclei polarization effects are not taken into account, so the nuclear spins \mathbf{I}_n are randomly oriented. As a result, Ω_N is also a random quantity that may be described by the Gaussian distribution function.

$$\mathcal{F}(\Omega_N) = \sqrt{\frac{2}{\pi}} T_2^* e^{-2(\Omega_N T_2^*)^2}, \quad (5)$$

where the reverse dephasing time [21]

$$\frac{1}{T_2^*} = \frac{v_0}{\hbar} \sqrt{\sum_n \frac{4}{3} I_n(I_n + 1) [A_h \Phi_h^2(\mathbf{R}_n) - A_e \Phi_e^2(\mathbf{R}_n)]^2}. \quad (6)$$

defines the random field dispersion: $\langle \Omega_N^2 \rangle = 1/(2T_2^*)^2$.

3. Polarized luminescence

Note that both the reverse radiative exciton lifetime τ_r^{-1} and the radiative doublet splitting $\delta_b = \hbar \Omega_{\perp} = \hbar \sqrt{\Omega_x^2 + \Omega_y^2}$ resulting from the long-range exchange interaction are proportional to the squared matrix element of optical exciton excitation, in particular, to squared wave function overlapping of the electron and hole in the real and momentum spaces [22]. Therefore, the overlapping integral is excluded in $\Omega_{\perp} \tau_r \equiv w_{QD}$. In the direct band gap quantum dot, this product may take arbitrary values from very high, $w_{QD} \gg 1$, to very low, $w_{QD} \ll 1$ depending on the anisotropic form of the quantum dot. Therefore, for indirect band gap quantum dots, such scatter of the values of w_{QD} is still possible. Here, the discussion is limited to the analysis of the most interesting case $w_{QD} \gg 1$, and the non-radiative recombination and spin relaxation not related to the hyperfine interaction are neglected [4].

Let's introduce the three-component vector $\mathbf{P}^{(0)}$ from the Stokes parameters $P_1^{(0)}$, $P_2^{(0)}$, $P_3^{(0)}$ [23] for radiation falling normally along z to the sample surface and the same vector \mathbf{P} for forward light emitted by the excitons. Indices 1, 2 and 3 are used here instead of l, l', c [2]. For a backward light configuration, the sign of P_3 characterizing the circular light polarization shall be reversed. When $w_{QD} \gg 1$, the Stokes parameter sets are interconnected by the following equation

$$P_i = \sum_{j=1,2,3} \Lambda_{ij} P_j^{(0)}, \quad (7)$$

where the coupling matrix [2] is

$$\Lambda_{ij} = \frac{\Omega_i \Omega_j}{\Omega^2} \quad (8)$$

and $\Omega^2 = \Omega_1^2 + \Omega_2^2 + \Omega_3^2$. Because the omnidirectional photoluminescence intensity doesn't depend on the exciting light polarization, this expression may be averaged over distribution (5) of the nuclear field Ω_N . For each individual quantum dot, the lateral x, y axes may be chosen in which $\Omega_2 = 0$ and $\Omega_{\perp} = \Omega_1 > 0$. Then non-zero components of the Stokes parameter coupling matrix read

$$\begin{aligned} \langle \Lambda_{11} \rangle &= 1 - \langle \Lambda_{33} \rangle = \int_{-\infty}^{\infty} \frac{\Omega_1^2 F(\Omega_N) d\Omega_N}{\Omega_1^2 + (\Omega_B + \Omega_N)^2} \\ &= \pi \Omega_1 T_2^* V(\Omega_B T_2^*; 1/2, \Omega_1 T_2^*), \end{aligned} \quad (9a)$$

$$\langle \Lambda_{13} \rangle = \langle \Lambda_{31} \rangle = \frac{\Omega_B}{\Omega_1} \langle \Lambda_{33} \rangle, \quad (9b)$$

where the Voigt distribution (or profile) is determined according to

$$V(u; \sigma, \gamma) = \int_{-\infty}^{\infty} \frac{e^{-v^2/(2\sigma^2)}}{\sigma\sqrt{2\pi}} \frac{1}{\pi} \frac{\gamma}{(u-v)^2 + \gamma^2} dv.$$

Thus, the photoluminescence polarization properties of an individual quantum dot are described by two dimensionless parameters $\Omega_1 T_2^*$ and $\Omega_B T_2^*$.

Magnetic field dependences of three non-zero matrix components $\langle \hat{\Lambda} \rangle$ are shown in the figure for three cases of (a) strong, $\Omega_1 T_2^* \gg 1$, and (b) weak, $\Omega_1 T_2^* \ll 1$, anisotropic splitting. In case (a), the hyperfine interaction is of minor importance and the magnetic field dependences are not much different from the limit dependences at $\Omega_N \rightarrow 0$ [22]:

$$\langle \Lambda_{11}(\Omega_N \rightarrow 0) \rangle = \frac{\Omega_1^2}{\Omega_1^2 + \Omega_B^2},$$

while $\langle \Lambda_{33}(\Omega_N \rightarrow 0) \rangle$ and $\langle \Lambda_{13}(\Omega_N \rightarrow 0) \rangle$ are expressed in terms of $\langle \Lambda_{11}(\Omega_N \rightarrow 0) \rangle$ using relations (9b). In case (b), the hyperfine interaction plays a leading part and equation (9a) is simplified to

$$\langle \Lambda_{11}(\Omega_1 \rightarrow 0) \rangle = \pi \Omega_1 F(\Omega_B).$$

Comparison with Figure 1a shows that the Overhauser field suppresses the optical alignment and enhances the optical orientation.

Let the x, y axis be rotated counterclockwise at ϕ with respect to the laboratory system of the x_0, y_0 axes. Then the coupling matrix $\langle \Lambda_{i_0 j_0} \rangle$ in the x_0, y_0 coordinates is related to the matrix components $\langle \Lambda_{ij} \rangle$ as follows

$$\begin{aligned} & \|\langle \Lambda_{i_0 j_0} \rangle\| = \\ & \begin{bmatrix} \langle \Lambda_{11} \rangle \cos^2 2\phi & \langle \Lambda_{11} \rangle \sin 2\phi \cos 2\phi & \langle \Lambda_{13} \rangle \cos 2\phi \\ \langle \Lambda_{11} \rangle \sin 2\phi \cos 2\phi & \langle \Lambda_{11} \rangle \sin^2 2\phi & \langle \Lambda_{13} \rangle \sin 2\phi \\ \langle \Lambda_{13} \rangle \cos 2\phi & \langle \Lambda_{13} \rangle \sin 2\phi & \langle \Lambda_{33} \rangle \end{bmatrix}. \end{aligned} \quad (10)$$

When all quantum dots in the array have coinciding lateral anisotropy axes, then expressions (9a), (9b) are applicable and shall be averaged with respect to the splitting distribution Ω_1 . If the lateral anisotropy axes are scattered randomly over the whole circumference, then, after averaging with respect to ϕ , only the diagonal components of the coupling matrix will remain non-zero.

$$\langle \langle \Lambda_{11} \rangle \rangle = \langle \langle \Lambda_{22} \rangle \rangle = \frac{1}{2} \langle \Lambda_{11} \rangle, \quad \langle \langle \Lambda_{33} \rangle \rangle = \langle \Lambda_{33} \rangle.$$

4. Exciton sublevel anticrossing with magnetic field growth

Now let's look at a stronger magnetic field at which energies of one of the dark excitons and one of the bright

excitons are compared, for example, with the projection of the angular momentum $+1$ [1]. In this case, the Overhauser field inducing small perturbation that reduces the system symmetry, nevertheless, leads to strong resonance mixing of the approaching levels, i.e. to their anticrossing, and affects considerably the luminescence intensity and polarization even for direct band gap quantum dots [24–28]. Anticrossing phenomenon due to the field B_N may be observed in the magnetic field $B_e^{(cr)} = \delta_0 / (2\mu_B |g_{e,\parallel}|)$ or $B_h^{(cr)} = \delta_0 / (2\mu_B |g_{h,\parallel}|)$ [1]. Let's consider a single quantum dot in the magnetic field $B_e^{(cr)}$ and show how, due to a nuclear field with the nonpolarized resonance excitation, exciton radiation from this dot becomes partially circularly polarized and changes its intensity compared with that of the non-resonance field $B \neq B_e^{(cr)}$.

When $B = B_e^{(cr)}$, sublevels with the projections of the angular momentum $+2$ and $+1$ may be taken as a two-level system (considering that $g_{e,\parallel} > 0$) with the Hamiltonian

$$\mathcal{H} = \hbar \Omega_N^e \mathbf{S}_e,$$

where

$$\Omega_N^e = \frac{v_0}{\hbar} A_e \sum_n \Phi_e^2(\mathbf{R}_n) \mathbf{I}_n,$$

and it is assumed that $A_{e,xx} = A_{e,yy} = A_e$.

Let's introduce the angle ϑ by defining it as

$$\cos \vartheta = \frac{\Omega_{N,z}^e}{|\Omega_N^e|}.$$

In the case of resonance by nonpolarized light, the radiation intensity I_{-1} of the exciton $|-1\rangle$ is proportional to the combination of the times $\tau_{nr} / [\tau_r(\tau_r + \tau_{nr})]$ and remains unchanged in the vicinity of the dot $B_e^{(cr)}$, while the exciton radiation intensity from the levels subjected to anticrossing depends on ϑ . Omitting the calculations, the final result is shown for the exciton radiation intensity I and degree of circular polarization P_c during the nonpolarized resonance excitation

$$I \propto \frac{\tau_{nr}}{\tau_r(\tau_r + \tau_{nr})} \frac{a + b \cos^2 \vartheta}{c - d \cos^2 \vartheta}, \quad (11)$$

$$P_c = \frac{\tau_r(2\tau_r + \tau_{nr})}{a + b \cos^2 \vartheta} \sin^2 \vartheta. \quad (12)$$

The following coefficients are introduced here

$$a = (2\tau_r + \tau_{nr})(3\tau_r + 2\tau_{nr}),$$

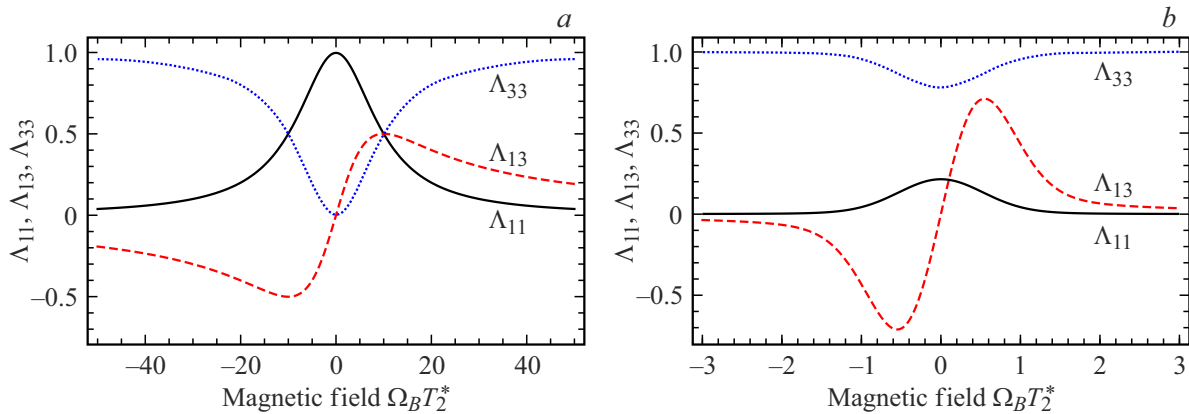
$$b = 2\tau_r^2 + \tau_r \tau_{nr} - 2\tau_{nr}^2,$$

$$c = (2\tau_r + \tau_{nr})^2, \quad d = \tau_{nr}^2,$$

that satisfy $a + b = 2(c - d) = 8\tau_r(\tau_r + \tau_{nr})$.

Similar to (6), the relaxation time $T_{2,e}^*$ is introduced:

$$\frac{1}{T_{2,e}^*} = \frac{v_0}{\hbar} \sqrt{\sum_n \frac{4}{3} I_n (I_n + 1) A_e^2 \Phi_e^4(\mathbf{R}_n)}. \quad (13)$$



Coefficients of linear coupling between the Stokes parameters of the exciting light and luminescence Λ_{11} (solid black curve), Λ_{13} (dashed red curve), Λ_{33} (dotted blue curve) calculated using equations (9) for $\Omega_1 T_2^* = 10$ (a) and 0.1 (b).

In real structures $\tau_{nr} \gg \tau_r$ [29], therefore the dimensionless parameter

$$\xi = \frac{\tau_r}{\tau_{nr}} \left(\delta_0 \frac{T_{2,e}^*}{\hbar} \right)^2$$

may be either greater or less than 1. Equations (11) and (12) are applicable when $\xi \gg 1$ [30], while, when $\xi \ll 1$, dynamic electron spin polarization is implemented [4]. Note that these studies provide, in particular, analytical expressions for averaged intensity and circular polarization in both limiting cases.

5. Conclusion

Besides the „bright-dark“ exciton δ_0 exchange splitting, epitaxial semiconductor quantum dots contain a smaller in magnitude exchange splitting of the bright exciton level δ_b resulting from the local lateral anisotropy of the structure. In indirect quantum dots, suppression of the long-range electron-hole exchange interaction contributes to the increasing role of the hyperfine interaction with the crystalline lattice nuclei in the exciton fine structure. This study investigates a special case of exciton fine structure in which the hyperfine interaction energy ε_N is low compared with δ_0 , but the relation between ε_N and δ_b is arbitrary. It is shown that nuclear spin fluctuations along the quantum dot structure growth axis in this mode lead to suppression of the optical alignment effect and enhancement of the optical orientation. Dependences of these effects on the longitudinal magnetic field are generally described by the Voigt profile. The effect of the Overhauser field on the radiation intensity and polarization in the region of magnetically-induced anticrossing of the bright and dark exciton sublevels is also examined.

Acknowledgments

The authors are grateful to A.V. Rodina for helpful discussion.

Funding

The study was funded by the Russian Science Foundation in the framework of project № 23-12-00142. D.S.S. is grateful to the Foundation for Development of Theoretical Physics and Mathematics „BAZIS“.

Conflict of interest

The authors declare that they have no conflict of interest.

References

- [1] E.L. Ivchenk, TT **60**, 1471 (2018) (in Russian). DOI: 10.21883/FTT.2018.08.46237.04Gr
- [2] D.V. Smirnov, E.L. Ivchenko, Phys. Rev. B **108**, 195432 (2023). DOI: 10.1103/PhysRevB.108.195432
- [3] J. Rautert, T.S. Shamirzaev, S.V. Nekrasov, D.R. Yakovlev, P. Klenovský, Yu.G. Kusrayev, M. Bayer, Phys. Rev. B **99**, 195411 (2019). DOI: 10.1103/PhysRevB.99.195411
- [4] D.S. Smirnov, T.S. Shamirzaev, D.R. Yakovlev, M. Bayer, Phys. Rev. Lett. **125**, 156801 (2020). DOI: 10.1103/PhysRevLett.125.156801
- [5] N. Akopian, N.H. Lindner, E. Poem, Y. Berlatzky, J. Avron, D. Gershoni, B.D. Gerardot, P.M. Petroff, Phys. Rev. Lett. **96**, 130501 (2006). DOI: 10.1103/PhysRevLett.96.130501
- [6] A. Dousse, J. Suffczynski, A. Beveratos, O. Krebs, A. Lemaître, I. Sagnes, J. Bloch, P. Voisin, P. Senellart, Nature **466**, 217 (2010). DOI: 10.1038/nature09148
- [7] D. Huber, M. Reindl, S.F. Covre da Silva, C. Schimpf, J. Martin-Sanchez, H. Huang, G. Piredda, J. Edlinger, A. Rastelli, R. Trotta, Phys. Rev. Lett. **121**, 033902 (2018). DOI: 10.1103/PhysRevLett.121.033902
- [8] F.T. Østfeldt, E.M. González-Ruiz, N. Hauff, Y. Wang, A.D. Wieck, A. Ludwig, R. Schott, L. Midolo, A.S. Sørensen, R. Uppu, P. Lodahl, PRX Quantum **3**, 020363 (2022). DOI: 10.1103/PRXQuantum.3.020363
- [9] O. Gühne, G. Tóth, Phys. Rep. **474**, 1 (2009). DOI: 10.1016/j.physrep.2009.02.004
- [10] C. Schimpf, M. Reindl, B.B. Francesco, K.D. Jöns, R. Trotta, A. Rastelli, Appl. Phys. Lett. **118**, 100502 (2021). DOI: 10.1063/5.0038729

- [11] T. Kuroda, T. Mano, N. Ha, H. Nakajima, H. Kumano, B. Urbaszek, M. Jo, M. Abbarchi, Y. Sakuma, K. Sakoda, I. Suemune, X. Marie, T. Amand, *Phys. Rev. B* **88**, 041306(R) (2013). DOI: 10.1103/PhysRevB.88.041306
- [12] D. Huber, M. Reindl, Y. Huo, H. Huang, J.S. Wildmann, O.G. Schmidt, A. Rastelli, R. Trotta, *Nat. Commun.* **8**, 15506 (2017). DOI: 10.1038/ncomms15506
- [13] C. Schimpf, F.B. Basset, M. Aigner, W. Attenender, L. Ginés, G. Undeutsch, M. Reindl, D. Huber, D. Gangloff, E.A. Chekhovich, C. Schneider, S. Höfling, A. Predojević, R. Trotta, A. Rastelli, *Phys. Rev. B* **108**, L081405 (2023). DOI: 10.1103/PhysRevB.108.L081405
- [14] R.I. Dzhioev, H.M. Gibbs, E.L. Ivchenko, G. Khitrova, V.L. Korenev, M.N. Tkachuk, B.P. Zakharchenya, *Phys. Rev. B* **56**, 13405 (1997). DOI: 10.1103/PhysRevB.56.13405
- [15] S.V. Gupalov, E.L. Ivchenko, A.V. Kavokin, *Proc. Int. Symp. „Nanostructures: Physics and Technology“*, St. Petersburg, 1996, pp. 322–325; **23**, 1205 (1998). DOI: 10.1006/spmi.1996.0367
- [16] D. Gammon, E.S. Snow, B.V. Shanabrook, D.S. Katzer, D. Park, *Phys. Rev. Lett.* **76**, 3005 (1996). DOI: 10.1103/PhysRevLett.76.3005
- [17] E.L. Ivchenko, *Phys. Status Solidi A* **164**, 487 (1997). DOI: 10.1002/1521-396X(199711)164:1;487::AID-PSSA487;3.0.CO;2-1
- [18] S.V. Gupalov, E.L. Ivchenko, A.V. Kavokin, *ZhETF* **113**, 703 (1998) (in Russian).
- [19] R.M. Stevenson, R.J. Young, P. See, D.G. Gevaux, K. Cooper, P. Atkinson, I. Farrer, D.A. Ritchie, A.J. Shields, *Phys. Rev. B* **73**, 033306 (2006). DOI: <https://doi.org/10.1103/PhysRevB.73.033306>
- [20] M.M. Glazov, E.L. Ivchenko, O. Krebs, K. Kowalik, P. Voisin, *Phys. Rev. B* **76**, 193313 (2007). DOI: 10.1103/PhysRevB.76.193313
- [21] M.M. Glazov, *Electron & Nuclear Spin Dynamics in Semiconductor Nanostructures* (Oxford University Press, Oxford, 2018).
- [22] E.L. Ivchenko, *Optical Spectroscopy of Semiconductor Nanostructures* (Alpha Science International, Harrow, UK, 2005).
- [23] L.D. Landau, E.M. Lifshits. *Teoriya polya*. (Fizmatlit, 2020) (in Russian).
- [24] Y. Masumoto, K. Toshiyuki, T. Suzuki, M. Ikezawa, *Phys. Rev. B* **77**, 115331 (2008). DOI: 10.1103/PhysRevB.77.115331
- [25] H. Kurtze, D.R. Yakovlev, D. Reuter, A.D. Wieck, M. Bayer, *Phys. Rev. B* **85**, 195303 (2012). DOI: 10.1103/PhysRevB.85.195303
- [26] D. Cogan, O. Kenneth, N.H. Lindner, G. Peniakov, C. Hopfmann, D. Dalacu, P.J. Poole, P. Hawrylak, D. Gershoni, *Phys. Rev. X* **8**, 041050 (2018). DOI: 10.1103/PhysRevX.8.041050
- [27] A.N. Starukhin, D.K. Nelson, B.S. Razbirin, D.L. Fedorov, D.K. Syunyaev, *FTT* **57**, 1888 (2015) (in Russian).
- [28] K.N. Boldyrev, M.N. Popova, B.Z. Malkin, N.M. Abishev, *Phys. Rev. B* **99**, 041105 (2019). DOI: 10.1103/PhysRevB.99.041105
- [29] T.S. Shamirzaev, A.V. Shumilin, D.S. Smirnov, J. Rautert, D.R. Yakovlev, M. Bayer, *Phys. Rev. B* **104**, 115405 (2021). DOI: 10.1103/PhysRevB.104.115405
- [30] A.V. Shumilin, T.S. Shamirzaev, D.S. Smirnov, *Phys. Rev. Lett.* **132**, 076202 (2024). DOI: 10.1103/PhysRevLett.132.076202

Translated by E.IIinskaya